Estimation of Power System Inertia from Ambient Wide Area Measurements

Kaur Tuttelberg, *Student Member, IEEE*, Jako Kilter, *Senior Member, IEEE*, Douglas Wilson, and Kjetil Uhlen, *Member, IEEE*

***Abstract*—This study presents a method of estimating the effective inertia of a power system from ambient frequency and active power signals measured by PMUs. Most importantly, we demonstrate that inertia can be estimated from ambient measurement data, not only from disturbances. This leads to the possibility of monitoring inertia in a close to continuous manner in the time scale of minutes or tens of minutes. The method allows the system to be divided into a number of areas and the effective inertia of each area to be estimated as a separate quantity. In principle, inertia is estimated by observing the dynamics between changes in active power and resulting frequency deviations during normal operation of the system. The method is based on applying system identification on these measurements and extracting inertia values from identified models. Efficacy of the method is demonstrated on results of real measurements from the Icelandic power system.**

***Index Terms*—Frequency control, Frequency dynamics, Inertial response, Phasor measurement units, Wide area monitoring**

I. Introduction

THE INCREASING share of power generating units connected to the system through power electronics is displacing synchronous generation. Larger penetration of renewable sources is both decreasing inertia [1]–[3] and changing its distribution in the system, leading to formation of low inertia areas [4], [5]. The associated challenges have been acknowledged and investigated in North America [1], [2], [6]–[8], Europe [3], [4], [9], Australia [10], [11], and elsewhere [5]. Some of the important arising questions are determining and monitoring values of inertia [2], [3], [9], considering the time varying nature of inertia [4], [12], and areas with low inertia [4], [5]. This study presents a method of estimating the inertia of different areas of the power system from ambient PMU measurements of active power and frequency. For a transmission system operator (TSO), the main requirement for monitoring the effective inertia of the system (or areas of it) is to estimate the time available to deploy a response, and to define the sensitivity between a frequency change and an appropriate corrective power response [2], [13].

K. Tuttelberg and J. Kilter are with the Department of Electrical Power Engineering and Mechatronics, Tallinn University of Technology, Tallinn, Estonia (e-mail of corresponding author: kaur.tuttelberg@ttu.ee).

D. Wilson is with GE Grid Solutions, Edinburgh, United Kingdom.

K. Uhlen is with the Department of Electric Power Engineering, Norwegian University of Science and Technology, Trondheim, Norway.

This project has received funding from the European Union's Horizon 2020 research and innovation programme under grant agreement No 691800 (MIGRATE project).

With any attempt at estimating inertia in a power system it is important to discuss the definition of inertia, or in this case, *effective* inertia. Effective inertia defines the relationship between a change in the power balance of the system or area and the rate of change of frequency of that area, which differs from a more conventional interpretation of inertia related to physical spinning mass and inertia time constants. The majority of inertia in its conventional meaning is contributed by the physical spinning mass of synchronous generators, but there are other elements of the system that can contribute to the effective inertial response of the system [14] (and even more so in the future), e.g. voltage and frequency dependence of load and power electronic interfaces for generation, load, and storage. The method presented in this paper separates the system into areas and estimates the (effective) inertia of each area—area inertia—by observing the dynamics between active power and frequency changes.

The estimation of inertia from recorded disturbances has been researched and tested in recent years. Inertia values of single units [15], [16], system areas [17], [18], and entire systems [19], [20] have been derived from PMU measurements of frequency events. Inertia has also been approximated from other information, like statuses of generators or correlation with total demand [2], [3], [9]. However, no attempts of estimating inertia more continuously from ambient measurements have been demonstrated so far. Different related parameter and model identification methods have been presented, e.g. estimation of low-order dynamic equivalent models from PMU measurements has been proposed [21] and identification of governor models has been demonstrated on real PMU measurements [22], [23]. A previous paper from the authors presented a comparison of different system identification methods applied on similar measurement data as in this study [24].

The main complication in estimating inertia is that during normal operation, the inertial response of the system cannot readily be distinguished from frequency control, voltage control, electro-mechanical dynamics, and stabilizing actions. The proposed approach identifies a combined model of inertial response and primary control from measured ambient dynamics, circumventing this limitation. The inertia estimates are found by fitting a model to the observed dynamics and extracting parameters corresponding to inertia from the model. There is an inherent approximation in fitting the complex nonlinear behavior of a power system to such a model; however, the simplification provides practically useful information for contracting and deploying frequency controls, including fast frequency response.

In this study, the proposed method is demonstrated on the example of the Icelandic power system and has been tested on real measurement data from this system. The Icelandic system is a relatively small isolated island with scattered generation and good coverage of PMU measurements. The method has been applied on ambient wide area measurements as intended. The models identified in the process of area inertia estimation have been validated on recorded frequency events. Even though testing the method on simulated data would give direct information about the accuracy of results in a controlled environment, testing it on real measurement data is significantly better for demonstrating its feasibility in real world conditions.

The theoretical background of the problem is covered in section II. The specifics of system identification and extraction of inertia values is described in section III. Test calculations on the measurements from the Icelandic power system are presented in section IV and discussed in section V. Conclusions are given in section VI.

II. Theoretical Background

In order to discuss the proposed system identification, it is helpful to analyze a theoretical model of the dynamics we are interested in. In the following, a simplified model of the dynamics between active power and frequency is given. This is done in order to analyze what data is needed to identify a model for these kinds of dynamics. These models or these particular model structures will not be directly used in any estimations.

The dynamics between power and frequency during a short period of time following a power mismatch occurrence can be modelled by the swing equation. For a single generator i, the equation commonly used in power systems engineering is expressed as

$$\frac{\mathrm{d}f_i}{\mathrm{d}t} = \frac{P_{iM} - P_{iE}}{2H_i S_{in}} f_n, \tag{1}$$

where P_{iM} is the output mechanical power of the machine, while P_{iE} is its electrical load power, f_i is the electrical frequency, H_i the inertia constant, S_{in} rated apparent power, and f_n the rated steady state frequency of the system. The model excludes damping effects and mechanical power is usually assumed to be constant.

As an approximation, an equivalent equation can be applied to an area of a system (or an entire system). For the aggregated frequency immediately after a load change in an area j we write another form of the swing equation

$$\frac{\mathrm{d}f_j}{\mathrm{d}t} = \frac{P_{jM} - P_{jE}}{M_j} = \Delta P_j / M_j, \tag{2}$$

expressed in terms of M_j. In other publications, the quantity M_j has been defined in terms of angular frequency [25], [26], but in this paper, its value expressed for a single machine is $M_i = 2H_i S_{in}/f_n$, i.e. it is expressed in terms of frequency. In this paper, we assume this form of the swing equation and define the effective inertia of an area as a proportionality term between $\mathrm{d}f_j/\mathrm{d}t$ and ΔP_j, equivalent to M_j. It should be noted that if the effective inertia is deduced from observed dynamics between power and frequency, then, contrary to its conventional definition, this proportionality term may also include other effects, not only the inertia of synchronous machines.

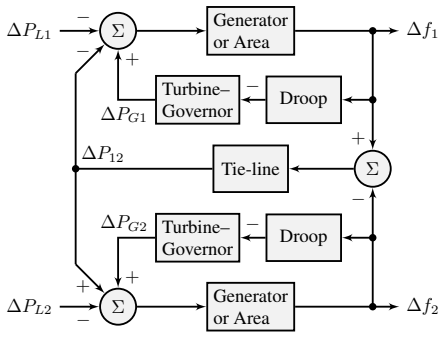

Fig. 1: Dynamic model of frequency control of a two-area power system with generator set-point changes disabled.

The inertia of a single synchronous machine is commonly represented by an inertia constant H, given in seconds. When several machines are lumped together, their inertia constants are weighted by the rated power of each machine. However, when observing the dynamics between active power and frequency, it is not practical to consider the rated power of every possible rotating machine and it is difficult to consider other possible effects contributing to the effective inertia. It is more convenient to use the single proportionality term M_j instead. By definition in the swing equation, it is effectively an angular momentum and its units are $\mathrm{J \cdot s}$ or $\mathrm{W \cdot s^2}$ [26].

Once the power mismatch event has occurred and frequency has started to deviate from its previous value, the frequency deviation is fed into a closed control loop, where governors counteract the power imbalance in the system. This control, mostly known as primary frequency control, but also frequency containment control, is carried out at the turbine–generator unit level. For a simpler analysis, we will look at this as a linear control system. The main components of a unit—the governor, the turbine, and the generator—are represented by corresponding transfer functions [27]. The inputs specify changes in the power set-point reference and load, while the output is the frequency deviation.

With a set of simplifications, an area of a power system (or an entire system) can be modeled similarly. In this case, the inertia of all rotating machines (and the frequency dependence of load) is lumped into a single area (or system) block and different governor–turbine systems are summed as parallel branches and lumped together by evaluating an equivalent droop. Based on that, a model for a multi-area interconnected system can be obtained by including tie-line elements that model the power exchanges between the areas [27]. The tie-lines are modeled as basic integrator blocks with a gain determined by line parameters.

This model can be simplified further when we analyze only primary frequency control, i.e. model the dynamics before any secondary control would be issued. In this case the power set-point values of generators remain unchanged and the corresponding inputs in the control system can be disregarded. A schematic of the model following that is given in Fig. 1, where

ΔP_{Li} are the changes in load of each area and $\Delta f_i = f_i - f_n$ the frequency deviations. In this simplified analysis of the dynamics of inertial response and frequency control, the multi-area system becomes a multi-input multi-output system with load changes as inputs and frequency changes as outputs.

The described model treats each area as a single node with aggregated load, generation, and control loops and a unified value of frequency. In such a model it is important to define areas that on a system level can be aggregated. The described treatment is also dependent on the possibility of analyzing the system in a period of time when the power set-points of all of the generators remain unchanged or change very little (i.e. $\forall i : \Delta P_{Ri} \approx 0$).

III. System Identification

It is proposed that once a power system has been divided into a number of appropriately defined areas, an approximate control system modelling the dynamics between frequency and active power can be identified. This is based on the assumption that the dynamics can be approximated as a linear control system with a structure that is in principle similar (but not necessarily identical) to the model discussed in the previous section (as in Fig. 1). During periods of time when generator set-points are not changed, the model can be assumed to have load changes as inputs and frequency deviations as outputs. If sufficient measurement data is available, it is possible to fit a model to the observed dynamics between the inputs and the corresponding outputs. Among other parameters, this model would include the inertia of each area.

A. Inputs and Outputs

The proposed methodology can only be applied on areas that are aggregated meaningfully, with two main requirements. The areas have to be consistent in terms of network topology—all nodes forming an area have to be directly connected to at least one other node of the area and areas have to be separable by clear boundaries. More importantly, the areas should consist of nodes that have frequencies close to each other. This is simple to understand with the example of inter-area oscillations, where the frequencies of the nodes in one area oscillate against the frequencies of the nodes forming another area. Knowledge about such areas in the power system can be used as a basis and analysis of measured frequency signals can be used to refine the separation into areas.

When an area is aggregated in order to model it similarly to the control system in Fig. 1, its center of inertia frequency is commonly used [26]. The center of inertia frequency is evaluated as a weighted average of frequencies

$$f_{\mathrm{COI}} = \frac{\sum_i^N H_i S_{in} f_i}{\sum_i^N H_i S_{in}}, \tag{3}$$

where f_i are the frequencies of all of the N nodes comprising the area weighted by the inertia of each node (nodes assumed to include no inertia are effectively excluded). Clearly, a degree of prior knowledge about inertia values of larger generators across the area is assumed when evaluating this quantity.

In this method, we use an aggregated area frequency that is a simplification of the center of inertia frequency. The frequency of area j is evaluated as a weighted average of measured frequencies

$$f_j = \frac{\sum_i^{N_j} w_i f_i}{\sum_i^{N_j} w_i}, \tag{4}$$

where f_i are the frequencies of the N_j nodes that are measured in area j. The weights w_i are picked based on analyzing the system and selecting frequency signals that reflect the general distribution of inertia in each area. The weights should consider which nodes contribute more to the inertia of the area but also consider its possible variability in time and the quality of frequency signals. In the simplest case, all nodes which are assumed to contribute some inertia are weighted equally and all other measured nodes weighted by zero.

R1 - 2.
R2 - 1.

In system identification, the input–output data can be pre-processed in different ways. It is common to subtract either the mean value or the first value of the time series, but sometimes the data is also detrended or processed in other ways [28]. Since we know the nominal value of frequency that the control system is attempting to achieve, it is possible to use the deviations from nominal frequency as the outputs. After evaluating the aggregated value, the frequency deviation in area j can be expressed as

$$\Delta f_j = f_j - f_n, \tag{5}$$

which is the jth output of the identified system.

Once the areas are formed and aggregated, it would be simple in principle to sum up all load changes in the areas to determine the inputs of the system. However, in order to do this directly, it would have to be possible to monitor the majority of load. Measuring load has not been the first priority when allocating PMU measurement resources and even if it becomes more common to monitor load feeders, it would take time until a sufficient share of them are covered. This means that more common PMU measurements have to be used to approximate the changes in load. When PMUs are installed in the system, they are most often set up to measure power flows on transmission lines, followed by monitoring of generators.

Fortunately, if power flows between the defined areas and a majority of generators that participate in primary frequency control can be monitored, it is possible to approximate load changes. The main assumption is that when small changes over time are considered, the changes in load and generation are sufficiently close to each other. The approximate change in load in area j would thus be

$$\Delta P_{Lj} \cong \sum_i \Delta P_{Gji} + \sum_k \Delta P_{Tjk} \tag{6}$$

where ΔP_{Gji} is the change in output power of the ith generator (or a group of generators) participating in primary frequency control in area j and ΔP_{Tjk} is the change in power transmitted from the kth to the jth area. All changes are evaluated with respect to the first value in the time series, i.e. $\Delta P = 0$ at $t = 0$.

In order to identify the dynamics between load changes and resulting frequency deviations it is necessary to monitor the

system for a sufficiently long period. Following a disturbance, the inertial response in frequency can be seen in the first few seconds, while the primary control (governor) response takes place in a time frame of tens of seconds. It can be assumed that a period of at least 1…2 minutes should be observed in order to capture enough variations in the system, but the period should not have to exceed 10 minutes. In practice, measurement periods of 2…6 minutes have been applied.

There are two main considerations to take into account while selecting the measurement periods. Firstly, these periods should exclude any time when automatic generation control (AGC) is acting or any other generator set-point changes are being made. A simple way to handle this is to consider the time these actions are executed and assume a buffer time for the associated effects to take place (e.g. 60 to 90 s). Secondly, it would be advisable to start and end the measurement periods at instances when area rate of change of frequency (i.e. $\mathrm{d}f/\mathrm{d}t$ or RoCoF) crosses zero. This is done in order to improve the efficiency of the system identification algorithm. This is relatively simple to implement even with noisy RoCoF measurements from PMUs.

B. System Identification

The next part of the estimation process is applying system identification on the obtained input–output data. Ambient load variations are generally small and they excite the dynamic system weakly. This means that a suitable system identification procedure is needed that is not sensitive to the low level of excitation. Some aspects of this problem have been studied in previous work, comparing various system identification methods applied in a similar way but with the example of analysing inter-area modes [24].

Regardless of which system identification method is used, a certain model order has to be specified. Even a small area of a power system contains many complicated control systems, making it very difficult to determine a correct order for such a model. However, most of the relevant dynamics of the system can be captured by a lower order model and the particular order itself may vary to some extent [24]. The order has to be large enough to capture the main dynamics but should still be small enough not to become too complicated or computationally expensive. In fact, it is possible to identify models of various orders from the same dataset and obtain a number of similar estimates [24].

The System Identification Toolbox in Matlab offers a selection of ready to use system identification tools and has been used in the presented method [28]. In a comparison of available identification algorithms, it was determined that the implementation of ARMAX is the best suited and most robust tool for the given type of problem [24]. The procedure presented in this paper uses this system identification method, but the general concept of area inertia estimation is not dependent on this particular implementation. Due to the complexity of identifying systems with many inputs and outputs, it would be recommendable to divide the system into 2…4 main areas of interest.

R1 - 1.

ARMAX in Matlab is a system identification technique based on the autoregressive–moving-average model with exogenous inputs. It results in a polynomial model, which is a generalized variant of a transfer function, expressing a relationship between an input, an output, and a noise term [28]. For a multi-input–multi-output (MIMO) ARMAX model with n_u inputs and n_y outputs, the input–output relationships for the lth output of the model can be expressed as

$$\sum_{j=1}^{n_y} A_{lj}(q)y_j(t) = \sum_{i=1}^{n_u} B_{li}(q)u_i(t-n_{ki}) + C_l(q)e_l(t), \quad (7)$$

where A_{lj}, B_{li}, and, C_l are polynomials of orders n_A, n_B, and n_C expressed in q^{-1}, and n_{ki} are the input–output delays in terms of number of samples. Polynomial models are discrete time (i.e. z-domain) linear systems and in this application the time step is determined by the sampling rate of PMU measurements.

R2 - 2.

Due to the nature of the system identification problem that was set up, the models have an equal number of inputs and outputs corresponding to the number of areas the system is divided into. As noted earlier, we apply system identification that attempts to fit a number of models in a range of orders $n = n_{\min}, \ldots, n_{\max}$ for each dataset. Within each iterated order, the various variables defining model order are equal, i.e. $n = n_A = n_B = n_C$. All input–output relationships are symmetric in the sense that in each identification attempt elements of the order matrices are equal. Input–output delays n_{ki} are determined with tools provided in Matlab once for a given system and assumed constant after that (a default value of zero is also sufficient in practice).

C. Inertia Estimation

Once we have identified approximate models describing the dynamics between load changes and frequency variations, it is still necessary to determine the effective inertia of each area. The ARMAX models include the effective inertia but not as an explicit value, thus, it is necessary to further analyze the identified models. A simple way to obtain results is to evaluate the step response of the ARMAX model and observe its initial slope. However, if sufficiently good models are identified, it is possible to extract inertia values from their parameters. One possible procedure for that is presented below.

First of all, the discrete time ARMAX models are converted into continuous time using the `d2c` function in Matlab. This is not successful in every case and the resulting models are checked once again for stability, this time with the s-domain criterion (real part of poles should be less than zero). The remaining polyniomial models are ready to be reduced to lower order transfer functions.

R2 - 2. covered

The continuous time models are reduced to a lower order using a set of functions available in Matlab. The models are first transformed into a balanced state-space realization. Next, insignificant states are identified and removed to form a reduced order system. The system is then transformed from the state-space representation into a continuous time transfer function. This is done using the `ssdata`, `balreal`, `modred`, and `ss2tf` functions in the System Identification Toolbox [29].

The expected structure of the transfer functions is of the generic form

$$H(s) = \frac{b_{n-1}s^{n-1} + b_{n-2}s^{n-2} + \ldots + b_0}{a_n s^n + a_{n-1}s^{n-1} + \ldots + a_0}. \quad (8)$$

The `ss2tf` tends to give marginal but non-zero values for the term b_n, resulting in the same dynamics but a different formal structure. In order to simplify the estimation of the effective inertia values, these b_n terms are set to zero in the presented implementation.

To understand how the effective inertia can be determined, we can look at a simplified example. If we have a single unit with no governor or frequency control, we can model the swing equation as a first order transfer function

$$H(s) = \frac{1}{Ms + D} = \frac{1/M}{s + D/M}, \quad (9)$$

where M is the effective inertia and D is frequency dependence of load [27]. The unit impulse response of this system is given by

$$h(t) = \frac{1}{M} \exp\left(-\frac{D}{M}t\right). \quad (10)$$

Clearly, instantly after the perturbation, at $t = 0$, the impulse response is equal to the inverse of the effective inertia. More precisely, the initial response of the system to a load disturbance is what we consider to be the effective inertia. Because we use load changes as inputs, the proportionality term is negative, i.e. $h(0) = -1/M$.

The identified transfer functions are more detailed than the single machine model without controls. However, the inertial response is still the fastest acting and we can assume that it determines the first instance of the impulse response. This means that the inertia of each area can be determined by the value of its unit impulse response at $t = 0$. For a transfer function with the structure given in (8), the estimates—i.e the first value of the impulse response—can be evaluated either with the `impulse` function, as the gain value of the zero-pole model from `tf2zpk` or most simply as the ratio of a_n to $-b_{n-1}$.

R2 - 4.

In the MIMO model it is also possible to determine the impulse response of the system, which provides an additional estimate of total system inertia (in addition to the sum of area inertia values). This is based on the principle that system COI frequency is an average of area frequencies weighted by the inertia of each area. Once area inertia values have been determined, it is possible to calculate system inertia from the unit impulse response of the whole system.

R1 - 2.

Based on responses of all N areas to a unit impulse in area k, the system inertia can be expressed as

$$M_{Sk} = -\frac{\sum_{i=1}^{N} 1/h_{ii}(0)}{\sum_{i=1}^{N} h_{ki}(0)/h_{ii}(0)}, \quad (11)$$

where $h_{ki}(0)$ is the response of the ith output of the MIMO system at time $t = 0$ to a unit impulse in the kth input. The $1/h_{ii}(0)$ values correspond to the effective inertia of each area and weight the output frequency deviation of each area so that the sum corresponds to the system COI frequency. It has been observed that in practice these estimates tend to have a lower variance than the sum of area inertia values.

One of the important aspects of the presented method is that several estimates are obtained from one period of monitoring data. The multiple ARMAX models identified with various model orders provide a number of estimates for area inertia, which can then be averaged. However, there are commonly a few poorly identified models that introduce outliers far from a realistic inertia value, which have to be detected and removed.

We propose to use the median absolute deviation (MAD), a robust median based statistic, defined as [30]–[32]

$$s_{\mathrm{MAD}}(X) = c\,\mathrm{med}\big(|X - \mathrm{med}(X)|\big), \quad (12)$$

where $\mathrm{med}(X)$ denotes the median of a sample $X = \{x_i \,|\, i = 1, \ldots, n\}$, x_i are the values in that sample, and c is a term introduced to achieve consistency with the standard deviation of a certain distribution [31]. Any value x_i for which

$$\frac{|x_i - \mathrm{med}(X)|}{s_{\mathrm{MAD}}(X)} > k \quad (13)$$

is considered an outlier and discarded. The cut-off factor k is chosen in conjunction with c and the assumed distribution. If a normal distribution is assumed, c takes the value of 1.4826 and k can be set to 2 for a 95% interval and 3 for a 99% interval [31].

IV. Test Calculations

A. Test System

The method has been tested on the Icelandic power system. The Icelandic system is a relatively small island system with a typical load around 1…2 GW and total installed generating capacity of 3 GW. In present terms, the system has a large number of PMU measurement points relative to its size, with more than 30 PMUs and around 200 measured voltage and current signals. A simplified schematic of the system is given in Fig. 2. The schematic includes all significant buses, generators, and lines and four large industrial loads, denoted by ILA, ILB, ILC, and ILZ. Total MVA ratings of power plants are given next to the symbols. The transmission system operator did not have a method of estimating or monitoring inertia at the time of this study.

Generators colored black in Fig. 2 are monitored directly by PMUs, i.e. their power flows are measured. However, generators in blue are not monitored yet and their output power flows are approximated. The simpler approximations are that the power flows on lines LA1, LF1, VF1, and SP2 are used as power measurements of the generators at LAX, LAG, VAF, and MJO respectively. Power flows on lines SN1 and FI2 are used to approximate the changes in generation at SVA and REY, units in the smaller area bounded by the blue dashed line. Additionally, all of the generation in the larger area bounded by the blue dashed line is approximated by power flows into or out of that area. These approximations may affect the accuracy of the results, but are sufficient to enable the application of this method.

The system has two main load centers, one in the west and one in the east. In terms of centers of inertia (COI), the

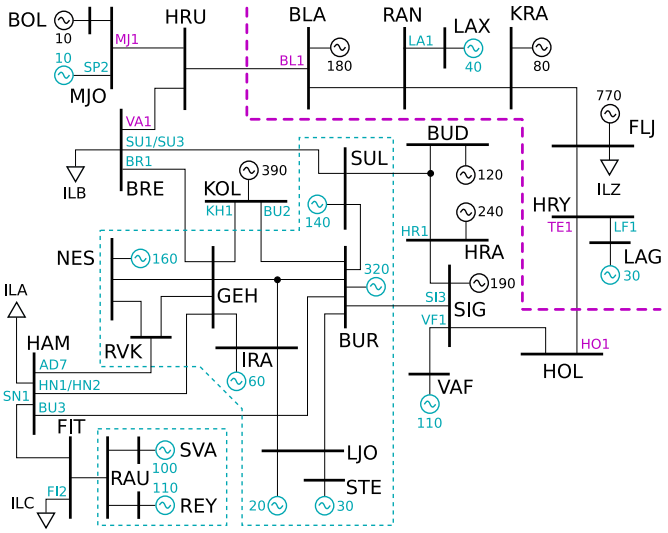

Fig. 2: Simplified schematic of the Icelandic power system. Larger black labels denote substations, smaller colored labels denote transmission lines. Total rated MVA of all generators at each plant given next to symbol.

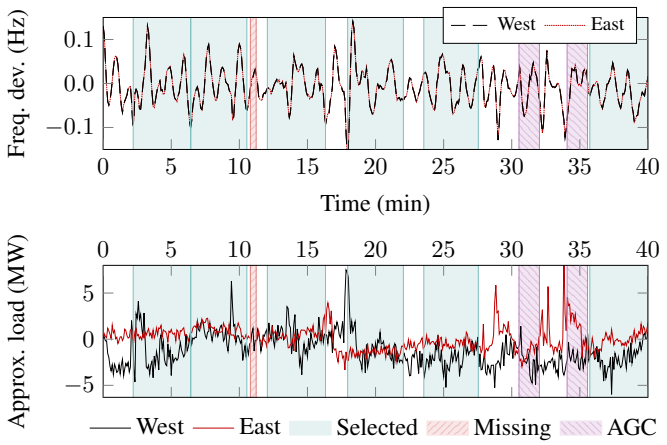

Fig. 3: Example of monitoring data used for the estimation of effective area and system inertia. Frequency deviations and load, approximated as in (6), plotted for the western and eastern areas. Six selected measurements, periods with missing data, and AGC operation marked by shaded areas.

R2 - 3.

system can be split quite naturally from the two long lines that connect these two areas, even though border nodes can deviate somewhat from their assigned area. The purple dashed line in Fig. 2 shows this split. Line labels written in purple denote the power flow measurements used to calculate area boundary power flows. Load variations are approximated based on (6), including the approximations used to find changes in power generated by the units that are not monitored.

Frequencies at KOL, SIG, HRA, and BUD were used for the western part and weighted by 1.5, 1.0, 1.0, and 0.5, and FLJ, KRA, and BLA were assigned to the eastern part with weights of 3.0, 1.0, and 0.5, respectively. The weight of BLA was set lower because it is a border node and its frequency differs more from frequencies of other nodes. These weights apply to area COI frequencies, not a whole system COI frequency. Frequency deviations were calculated for the aggregated areas using (4) and (5). It has been observed that in practice such an approach to evaluating area frequency and estimating effective area inertia is not very sensitive to the weights, meaning that crude assumptions are sufficient.

R2 - 2.

B. Validation of Method

The method was validated on a combination of measurements from both ambient conditions and frequency disturbances. The effective area inertia values were estimated from ambient measurements using the presented method. These measurements were gathered from time periods preceding frequency disturbances, meaning that the inertia values were estimated right before the events. The disturbances were then used to analyze the performance of the method. A total of 16 events were selected for the study, 14 of these were load trips (industrial loads at either ILA, ILB or ILC) and two were generator trips. Only so-called "clean" events were selected, i.e. disturbances where a single unit tripped at a moment when the system could be considered to be in steady-state and no other disturbance followed immediately. All disturbances took place in the western part of the system.

The accuracy of estimated inertia values was quantified by a comparison of the RoCoF of the recorded event and the corresponding RoCoF predicted from the inertia value for the given disturbance. From the disturbances, RoCoF was estimated as the slope of a linear fit to measured frequency during the period of 0.2 to 0.4 s after the trip. The jump in frequency is a measurement effect of the disturbance causing a step change in voltage phase angle, which cleared in 160 ms in most cases but an additional 2 cycle margin was assumed. The change in load, i.e. ΔP, was determined from the measured power at the tripped unit as the largest deviation during the first 0.3 s after the trip.

System identification was applied so that ARMAX models of orders 9 to 28 were identified, i.e. 20 models with different model orders. In each case with six consecutive measurement periods, the first identification was made with five iterations and each following made with three iterations using the results of the previous measurement as a starting point. The least squares non-linear fitting method was used inside the ARMAX routine and the input–output delay was set to zero. Identified models were reduced to 4th order transfer functions. MAD based outlier detection assumed a normal distribution and a 95% confidence interval.

C. Inertia Estimation Results

In order to explain the application of the method better, a little over 40 minutes of monitoring data is presented in Fig. 3 as an example of input data. From this longer period, six smaller sets of measurement data were selected by a preprocessing algorithm. In the algorithm, a minimum length (4 min in this case) was specified and measurement periods were selected so that they started and ended at $\mathrm{d}f/\mathrm{d}t = 0$, while avoiding moments when data was missing or AGC was operating. All of this is from ambient conditions, preceding a load trip that took place 42 minutes after the start of monitoring.

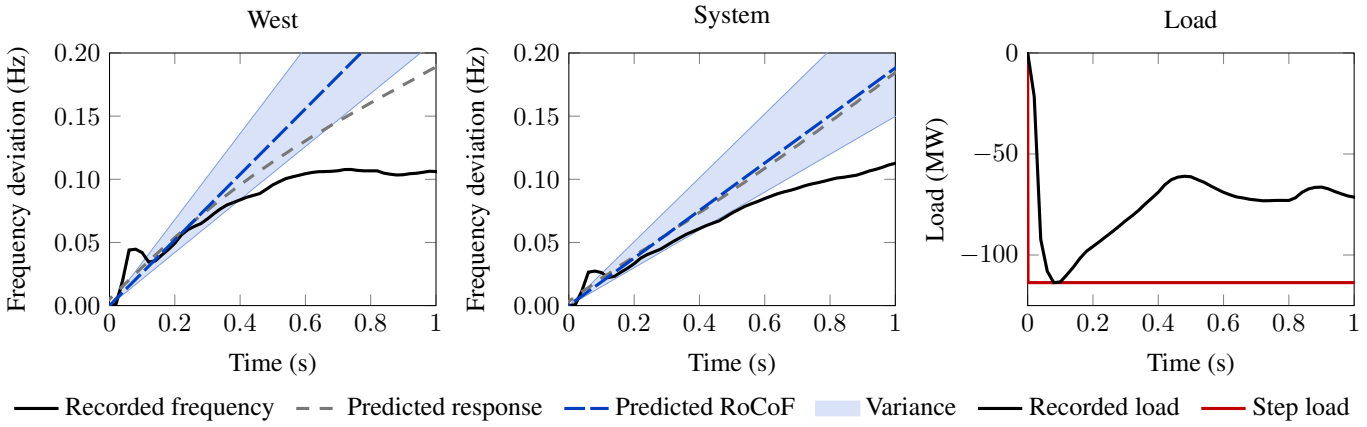

Fig. 4: Details of validation with event number 16. Measured COI frequency in the western area and entire system plotted in left and center graphs, alongside the responses predicted by the identified models and RoCoF slopes predicted from estimated inertia. Predictions were based on pre-event ambient data. Variance in predicted RoCoF based on two standard deviations of all inertia values given as shaded area. Rightmost graph shows the measured power at the tripped unit and the equivalent step signal used as the input of identified models. The magnitude of the step was also used as the ΔP when predicting RoCoF.

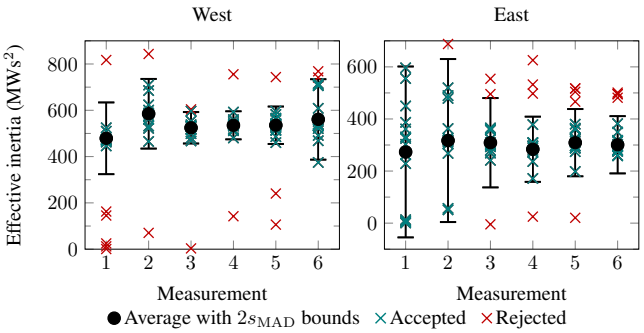

Fig. 5: Individual inertia estimates from the six measurements. Average inertia for each measurement is plotted, alongside all accepted values and outliers that were rejected based on the MAD criterion.

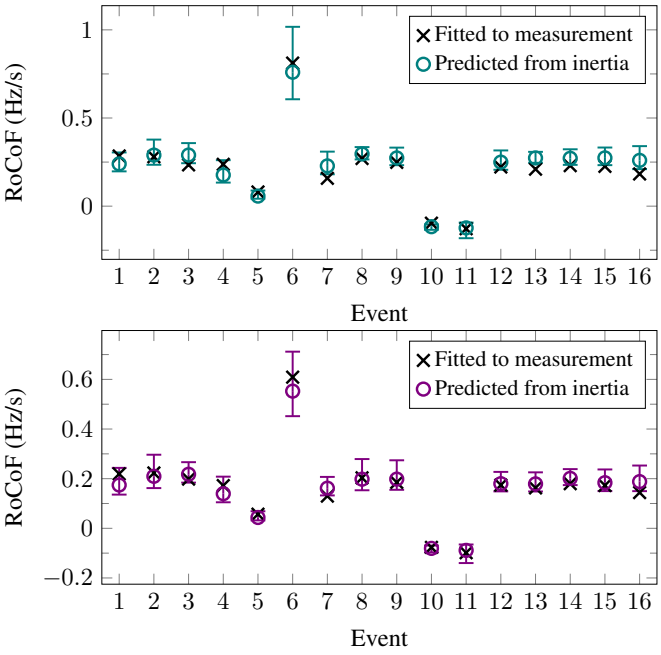

Fig. 6: Comparison of approximate RoCoF after each disturbances and corresponding RoCoF predicted from estimated inertia values for the western area (top) and the entire system (bottom). Variance bounds based on two standard deviations of all inertia samples of each case.

The main results of the method are presented in Fig. 5, where estimates of inertia from each measurement period are plotted. The figure shows individual estimates extracted from individual models and presents which values were accepted and which rejected as outliers. It also gives the average inertia value estimated from each measurement and shows the bound based on the MAD method that was used to detect outliers.

Following that, the results of the six measurements before the disturbance were further combined, decreasing variance in the estimates of inertia. The value of effective inertia estimated from the ambient monitoring data was then used to predict the RoCoF of the following frequency disturbance in each of the 16 cases. However, the cases were also analyzed in detail in order to validate the results more thoroughly. For this, the recorded frequency excursions were visually compared to predictions from the identified models and a RoCoF slope based on the estimated inertia. Recorded power of each tripped unit was used to determine the amount of load or power lost in the event. Fig. 4 presents this kind of validation of the case that showed the largest difference between predicted and comparison RoCoF values (area and system combined).

R2 - 6.

Measurements from all 16 cases were processed with the proposed method and effective inertia of the western part and the entire system were estimated. However, there were no reference values of inertia with known accuracy available to compare them to. In order to analyze the overall performance of the method, RoCoF values were compared instead. For each event, a RoCoF value and the amount of load (or generation) lost were estimated from the PMU measurements. The inertia values estimated from ambient measurements before the events were used to predict RoCoF values of corresponding disturbances.

A comparison of these results over all 16 cases are presented in Fig. 6 for the western area and the whole system. (No suitable validation events occurred in the eastern part of the system.) Differences between RoCoF values estimated from recorded frequencies and predicted from inertia values are

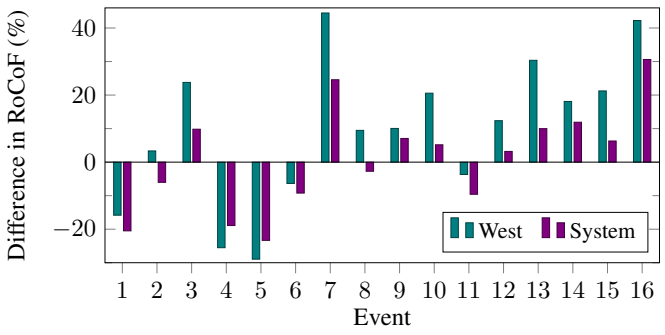

Fig. 7: Differences between approximate RoCoF and the corresponding value predicted from estimated inertia. Per cent difference of prediction from approximate RoCoF is given.

presented in Fig. 7. The average difference was 20% for the western area and 12% for the whole system. However, these should not be seen strictly as errors, since the RoCoF and ΔP values of the events were also approximated. For example, in validation event 16 shown in Fig. 4, the the first swing in the frequency of the western area started before 0.3 s, meaning the linear fit between 0.2 and 0.4 s was incorrect.

R2 - 6.

In computation time, processing one measurement period took around 20…50% of its length using a single core on a regular office laptop (Core i5-4200U@1.6 GHz, 12GB RAM). If the total length of all measurement periods in all 16 cases was 380 min then the total time the code took to process all of it was 140 min. On average it took 22 s to analyze one minute of monitoring data or 37% of its length.

V. Discussion

The method is based on first identifying the combined inertial and primary control response of the system and then extracting the value of inertia. This means that in order to find a good estimate of inertia, it is necessary that the inertial response is captured well enough in the identified system. The inertial and primary control responses can only be clearly separated in case of a distinct frequency disturbance. For these reasons, the models identified from ambient measurements were validated by comparing their inertial responses to recorded frequency disturbances.

Results of system identification were validated this way in all 16 cases. However, it is very difficult to quantify the quality of a model in this comparison. A scalar difference between the recorded and predicted time series could not consider the different dynamics in the system and was not suitable in many cases. Neither auto-correlation nor prediction error analysis could reliably describe the quality of identified models. Therefore, this type of validation was made as a visual comparison, with one example given in Fig. 4.

R2 - 5.

It was seen in the estimates of inertia (Fig. 5, measurements 1 and 2 of eastern area) that some results are clearly incorrect. The method is based on averaging a large number of estimates and detecting and removing outliers is an important part of that. While the MAD based outlier detection was suitable in most cases, in the example presented in Fig. 5 measurements 1 and 2 for the eastern part of the system showed that it does not always perform ideally. However, for the bounds based on MAD to be very wide, there has to be a similar number of values that are clearly underestimating and overestimating the real value, meaning the average result is not significantly distorted as errors are canceled out.

It is nevertheless important to quantify the accuracy of the method and in order to do that, a comparison of RoCoF values was carried out. It is possible to analyze a recorded frequency excursion and approximate a RoCoF value based on a linear fit during a certain period of the measurement. In this study, it was also possible to monitor the power of the tripped units and determine the change in load during the disturbance. Based on estimated inertia values, it was then possible to calculate another RoCoF value from the ratio of change in power to inertia. These two RoCoF values could be directly compared to each other as seen in Fig. 6 and Fig. 7.

Even though the reference RoCoF from each disturbance was also approximated and not correct in every case (e.g. event 16), this comparison over 16 different cases still offers insight into the expected accuracy of the method. The differences ranged from a few per cent up to around 40% in a few cases, with a 12% average in values for the entire system and 20% for the western area. A very important result is that considering variance bounds, not a single prediction underestimated the RoCoF value caused by the disturbance. Even though some estimated effective inertia values predicted a slightly lower RoCoF, the upper bound gave a sufficiently conservative value in each case.

The computational cost of the algorithm is considerable and the time taken to process one measurement period can be in the same order of magnitude as its length. In the presented results, it took 20…50% of the length of the measurement period. If an average monitoring period of 4 min was assumed, then an on-line application could give the average effective inertia of this period 5…6 min after the start of measurement. The bulk of the computational work could be run in parallel (every model order is independent) and significantly shorter running times could be achieved on a more powerful computer. On the other hand, increasing the number of input–output pairs would increase the computational burden.

VI. Conclusions

The paper presented a method of estimating the effective inertia of a system and its areas from ambient wide area measurements, i.e. during normal system operation. The developed method would enable a close to continuous and close to real-time monitoring of inertia. The method is based on identifying both the inertial response and primary frequency control in the dynamics between active power and frequency.

The most important result of the work is demonstrating that effective inertia can be monitored based on ambient measurements, not only frequency disturbances. Thus, a TSO can determine the time available to deploy frequency response before frequency thresholds are crossed and load is lost or other secondary disturbances occur. This means that the amount of fast-acting reserve can be identified and allocated per area of the power system, and the response time requirements specified. While there is sometimes a sizable spread in

estimates, it was possible to determine a conservative estimate to define the maximum expected RoCoF in every disturbance case.

VII. Acknowledgment

We would like to thank Landsnet, the Icelandic TSO for providing measurement data for the study, with special thanks to Ragnar Gudmansson and Birkir Heimisson. We would also like to acknowledge Colin Foote (SP Energy Networks) for helpful comments about the manuscript.

References

[1] V. Gevorgian, Y. Zhang, and E. Ela, "Investigating the impacts of wind generation participation in interconnection frequency response," *IEEE Transactions on Sustainable Energy*, vol. 6, no. 3, pp. 1004–1012, July 2015.

[2] S. Sharma, S. H. Huang, and N. Sarma, "System inertial frequency response estimation and impact of renewable resources in ERCOT interconnection," in *2011 IEEE Power and Energy Society General Meeting*, July 2011, pp. 1–6.

[3] E. Ørum, M. Kuivaniemi, M. Laasonen, A. Bruseth, E. Jansson, A. Danell, K. Elkington, and N. Modig, "Future system inertia," ENTSO-E Nordic Analysis Group, Tech. Rep., 2015.

[4] "Frequency stability evaluation criteria for the synchronous zone of continental Europe," ENTSO-E RG-CE System Protection & Dynamics Sub Group, Tech. Rep., March 2016.

[5] H. Pulgar-Painemal, Y. Wang, and H. Silva-Saravia, "On inertia distribution, inter-area oscillations and location of electronically-interfaced resources," *IEEE Transactions on Power Systems*, vol. 33, no. 1, pp. 995–1003, Jan 2018.

[6] J. Conto, "Grid challenges on high penetration levels of wind power," in *2012 IEEE Power and Energy Society General Meeting*, July 2012, pp. 1–3.

[7] N. W. Miller, M. Shao, S. Venkataraman, C. Loutan, and M. Rothleder, "Frequency response of California and WECC under high wind and solar conditions," in *2012 IEEE Power and Energy Society General Meeting*, July 2012, pp. 1–8.

[8] N. W. Miller, M. Shao, R. D'aquila, S. Pajic, and K. Clark, "Frequency response of the US Eastern Interconnection under conditions of high wind and solar generation," in *2015 Seventh Annual IEEE Green Technologies Conference*, April 2015, pp. 21–28.

[9] I. Dudurych, M. Burke, L. Fisher, M. Eager, and K. Kelly, "Operational security challenges and tools for a synchronous power system with high penetration of non-conventional sources," *CIGRE Science & Engineering*, vol. 7, February 2017.

[10] H. Gu, R. Yan, and T. K. Saha, "Minimum synchronous inertia requirement of renewable power systems," *IEEE Transactions on Power Systems*, vol. PP, no. 99, pp. 1–1, 2017.

[11] R. Yan, T. K. Saha, N. Modi, N.-A. Masood, and M. Mosadeghy, "The combined effects of high penetration of wind and PV on power system frequency response," *Applied Energy*, vol. 145, pp. 320 – 330, 2015.

[12] V. Trovato, I. M. Sanz, B. Chaudhuri, and G. Strbac, "Advanced control of thermostatic loads for rapid frequency response in Great Britain," *IEEE Transactions on Power Systems*, vol. 32, no. 3, pp. 2106–2117, May 2017.

[13] W. Li, P. Du, and N. Lu, "Design of a new primary frequency control market for hosting frequency response reserve offers from both generators and loads," *IEEE Transactions on Smart Grid*, vol. PP, no. 99, pp. 1–1, 2017.

[14] Y. Bian, H. Wyman-Pain, F. Li, R. Bhakar, S. Mishra, and N. P. Padhy, "Demand side contributions for system inertia in the GB power system," *IEEE Transactions on Power Systems*, vol. PP, no. 99, pp. 1–1, 2017.

[15] P. Wall and V. Terzija, "Simultaneous estimation of the time of disturbance and inertia in power systems," *IEEE Transactions on Power Delivery*, vol. 29, no. 4, pp. 2018–2031, Aug 2014.

[16] P. Wall, P. Regulski, Z. Rusidovic, and V. Terzija, "Inertia estimation using PMUs in a laboratory," in *IEEE PES Innovative Smart Grid Technologies, Europe*, Oct 2014, pp. 1–6.

[17] G. Chavan, M. Weiss, A. Chakrabortty, S. Bhattacharya, A. Salazar, and F. H. Ashrafi, "Identification and predictive analysis of a multi-area WECC power system model using synchrophasors," *IEEE Transactions on Smart Grid*, vol. 8, no. 4, pp. 1977–1986, July 2017.

[18] J. D. Lara-Jimenez, J. M. Ramırez, and F. Mancilla-David, "Allocation of pmus for power system-wide inertial frequency response estimation," *IET Generation, Transmission Distribution*, vol. 11, no. 11, pp. 2902–2911, 2017.

[19] P. M. Ashton, C. S. Saunders, G. A. Taylor, A. M. Carter, and M. E. Bradley, "Inertia estimation of the GB power system using synchrophasor measurements," *IEEE Transactions on Power Systems*, vol. 30, no. 2, pp. 701–709, March 2015.

[20] P. M. Ashton, G. A. Taylor, A. M. Carter, M. E. Bradley, and W. Hung, "Application of phasor measurement units to estimate power system inertial frequency response," in *2013 IEEE Power Energy Society General Meeting*, July 2013, pp. 1–5.

[21] M. Shiroei, B. Mohammadi-Ivatloo, and M. Parniani, "Low-order dynamic equivalent estimation of power systems using data of phasor measurement units," *International Journal of Electrical Power & Energy Systems*, vol. 74, pp. 134 – 141, 2016.

[22] D. T. Duong, K. Uhlen, and E. A. Jansson, "Estimation of hydro turbine-governor system's transfer function from PMU measurements," in *Power and Energy Society General Meeting, 2016 IEEE*, July 2016.

[23] S. H. Jakobsen and K. Uhlen, "Vector fitting for estimation of turbine governing system parameters," in *2017 IEEE Manchester PowerTech*, June 2017, pp. 1–6.

[24] K. Tuttelberg, J. Kilter, and K. Uhlen, "Comparison of system identification methods applied to analysis of inter-area modes," in *Proceedings of International Power Systems Transients Conference 2017*, Seoul, South Korea, June 2017.

[25] A. Ulbig, T. S. Borsche, and G. Andersson, "Impact of low rotational inertia on power system stability and operation," *IFAC Proceedings Volumes*, vol. 47, no. 3, pp. 7290 – 7297, 2014, 19th IFAC World Congress.

[26] P. M. Anderson and A. A. Fouad, *Power System Control and Stability, 2nd Edition*, M. E. El-Hawary, Ed. Wiley, 2002.

[27] P. Kundur, *Power System Stability and Control*. McGraw-Hill, 1993.

[28] *MATLAB and System Identification Toolbox R2016b: User's Guide*, The MathWorks, Inc., Natick, Massachusetts, 2016.

[29] L. Andersson, U. Jönsson, K. H. Johansson, and J. Bengtsson, "A manual for system identification," 2006.

[30] F. R. Hampel, "The influence curve and its role in robust estimation," *Journal of the American Statistical Association*, vol. 69, no. 346, pp. 383–393, 1974.

[31] P. J. Rousseeuw and C. Croux, "Alternatives to the median absolute deviation," *Journal of the American Statistical Association*, vol. 88, no. 424, pp. 1273–1283, 1993.

[32] C. Leys, C. Ley, O. Klein, P. Bernard, and L. Licata, "Detecting outliers: Do not use standard deviation around the mean, use absolute deviation around the median," *Journal of Experimental Social Psychology*, vol. 49, no. 4, pp. 764 – 766, 2013.